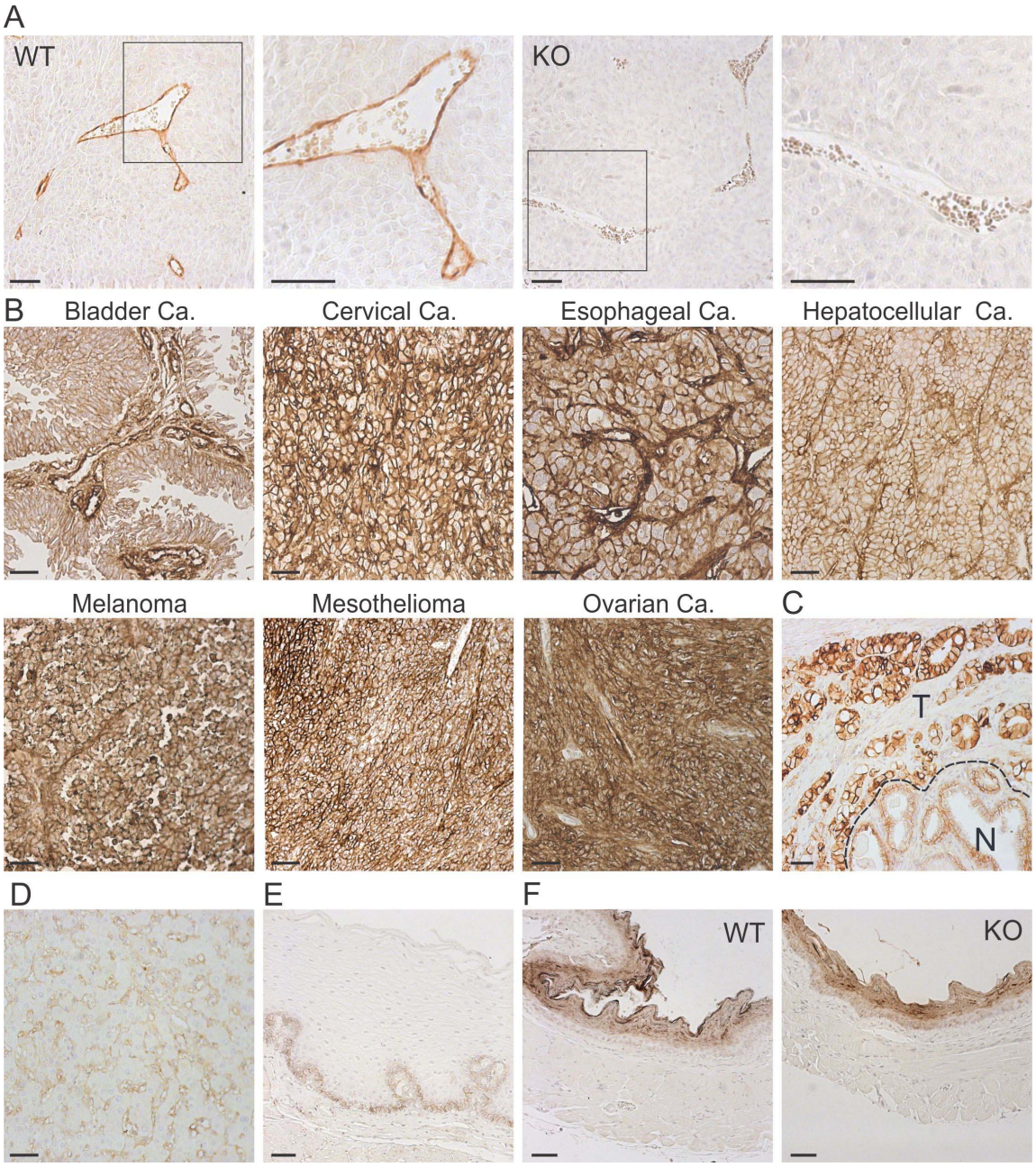

Figure S1, related to Figure 1. **(A)** The goat anti-human CD276 antibody used for IHC in Figure 1 (main text) was used to stain murine CD276 in FFPE sections of MC38 tumors. Note the absence of vessel staining in the *Cd276* KO mice. Red blood cells can be observed inside the vessels. **(B)** Representative examples of strong CD276 IHC staining of both tumor cells and tumor vasculature are shown for bladder cancer, cervical cancer, esophageal cancer, hepatocellular carcinoma, melanoma, mesothelioma and ovarian cancer. **(C)** CD276 immunostaining of human prostate adenocarcinoma adjacent to normal prostate tissue. Note the elevated CD276 in the tumor (T) region next to normal (N) prostate. **(D)** Although weak reactivity of the goat polyclonal CD276 antibody with sinusoidal endothelium was detectable by IHC in normal human liver (light brown stain), the absence of a similar staining pattern in murine liver (not shown) precluded specificity validation using *Cd276* WT versus KO mice. **(E)** CD276 immunostaining of human esophagus. Note the low level staining in the basal cells. **(F)** CD276 immunostaining of esophagus from *Cd276* WT and KO mice. Note the goat polyclonal anti-CD276 antibody reacts non-specifically with epithelial cells of the esophagus. The brown staining was absent from control sections stained with a non-specific goat IgG (not shown). Bars in (A) to (F): 50 μm.

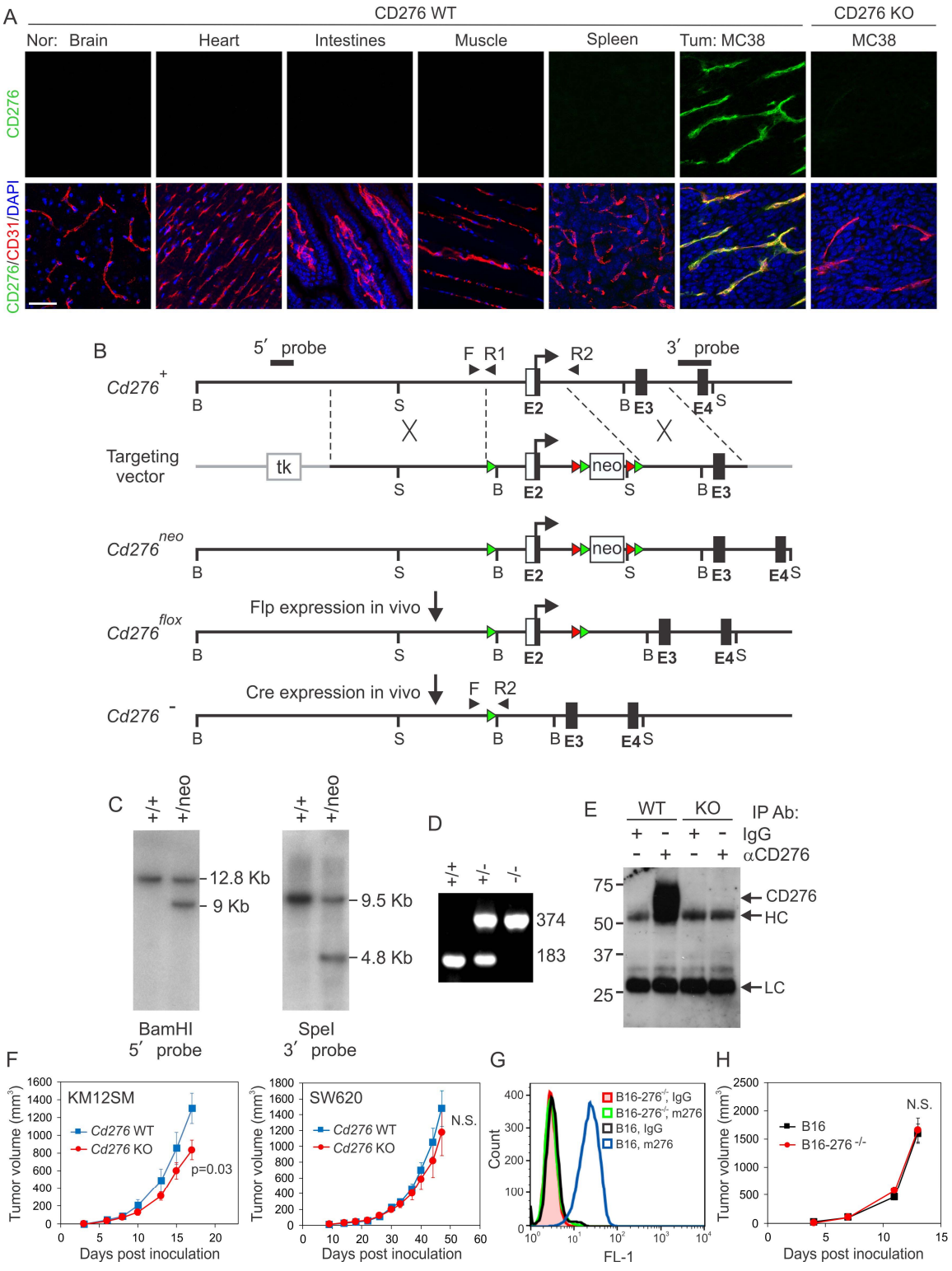

Figure S2, related to Figure 2. **(A)** CD276 IF staining of normal mouse organs from *Cd276* WT mice and MC38 tumors from *Cd276* WT and KO mice. Vessels were counterstained with CD31 (red). MC38 tumors from *Cd276* KO mice are included as a specificity control. Scale bar: 100 µm. **(B)** The targeting vector used to disrupt the *Cd276* locus was designed to incorporate lox-p sites (green triangles) on either side of exon 2 (E2) that contains the start codon and signal peptide (forward arrow). Frt sites (red triangles) were

incorporated on either side of the neomycin (neo) gene to facilitate removal of the neo cassette by crossing *Cd276*^{neo} mice with transgenic β-actin-flp mice. Mice with *Cd276* 'floxed' alleles (*Cd276*^{flox}) were crossed with β-actin-cre transgenic mice to generate offspring with a *Cd276* null allele. B: BamH1, S: SpeI. **(C)** Southern blots were used to identify the correctly targeted neo allele in ES cells. The 5' and 3' probes used for the Southern analysis are shown in (B). **(D)** PCR screen used for routine genotyping. The PCR reaction contained the three primers F, R1 and R2 indicated in (B) (black arrowheads). The WT allele is 184 bp and the KO allele is 374 bp. **(E)** CD276 protein was immunoprecipitated (IP) from MC38-276$^{-/-}$ tumors grown subcutaneously in either *Cd276* WT or KO mice using either a rabbit anti-CD276 mAb or a control rabbit non-specific IgG mAb. CD276 protein was detected by immunoblotting with a goat anti-CD276 mAb and was only detected in *Cd276* WT mice. HC: Heavy chain, LC: Light chain. **(F)** KM12SM or SW620 colon tumor cells were inoculated subcutaneously into athymic nude *Cd276* WT or KO mice and tumor growth monitored. n = 12/group (KM12SM), n = 13 (WT) or 9 (KO) per group (SW620). **(G)** Flow cytometry was used to verify the absence of CD276 in B16-276$^{-/-}$ tumor cells. **(H)** B16 or B16-276$^{-/-}$ tumor cells were inoculated subcutaneously into C57BL/6 mice and tumor growth monitored. N.S. Non-significant. n = 14 (B16) or 13 (B16-276$^{-/-}$) per group. Error bars in (F) and (H) represent SEM.

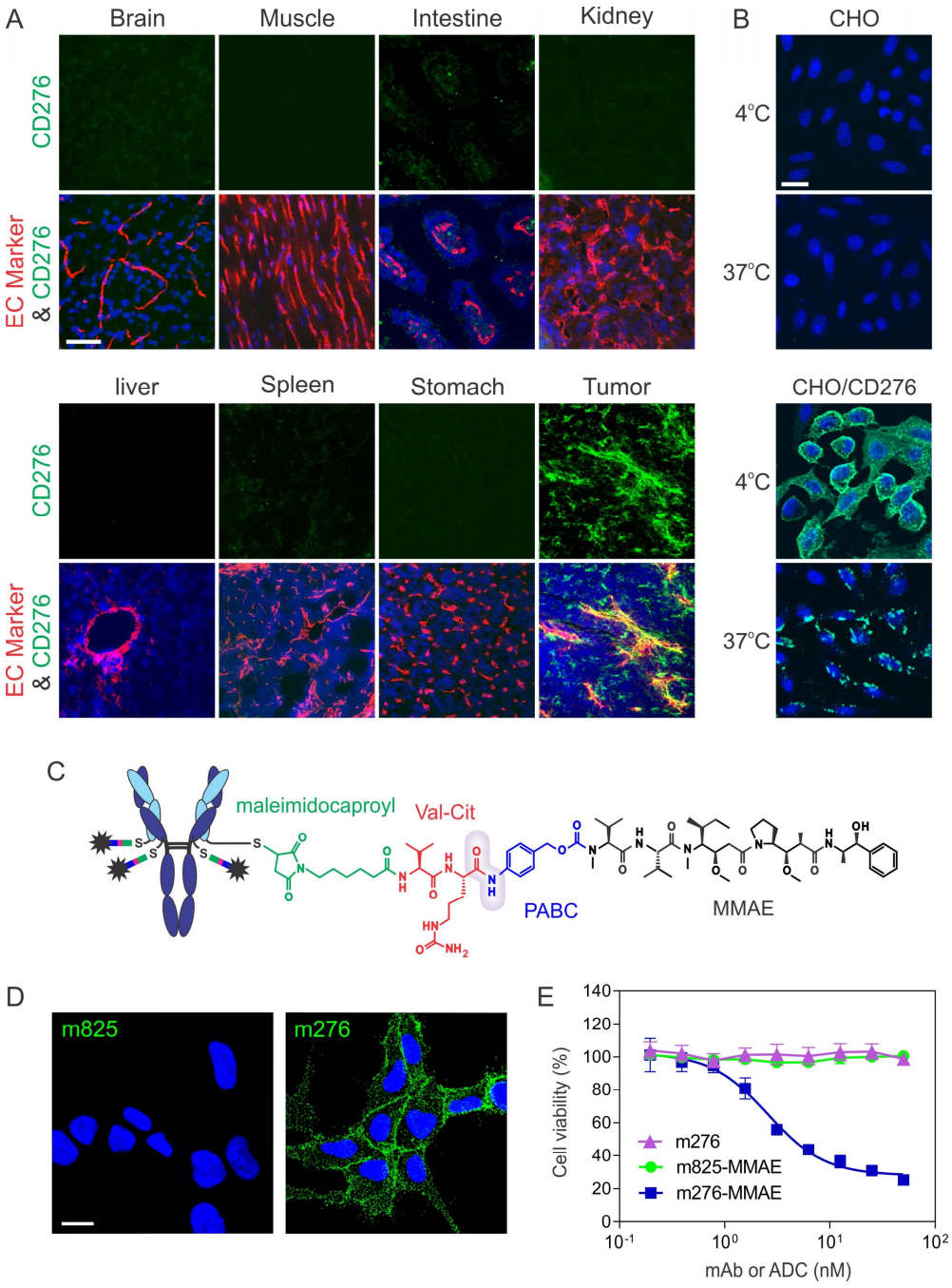

Figure S3, related to Figure 3. (A) IF staining to assess binding and localization of FITC-labeled m276 in various normal tissues and tumors (Pan02) 3 hours post i.v. injection. Tumor vessels were detected with a mixture of CD31 and PV-1 (Meca-32) antibodies (red). Nuclei were counterstained with DAPI (blue). Scale bar: 50µm. **(B)** The uptake of FITC-labelled m276 was evaluated in CHO or CHO/CD276 cells after shifting cells from 4°C to 37°C for 90 minutes. Scale bar: 20 µm. **(C)** Chemical structure of m276-MMAE linker and warhead. The maleimidocaproyl attachment group is in green, the p-aminobenzylcarbamate (PABC) spacer is in blue, and the cathepsin B cleavable valine-citrulline dipeptide is in red. The MMAE drug-linker was bound via disulfide linkages to free cysteines on m276. The grey cloud highlights the amide group susceptible to cleavage by carboxylesterase 1C in mouse serum. **(D)** CD276 (green) IF staining of 293 cells using m276 anti-CD276 mAb or a nontargeting mAb control (m825). Scale bar: 20µm. **(E)** 293 cell viability following treatment with m276, m825-MMAE and m276-MMAE. Error bars = SD.

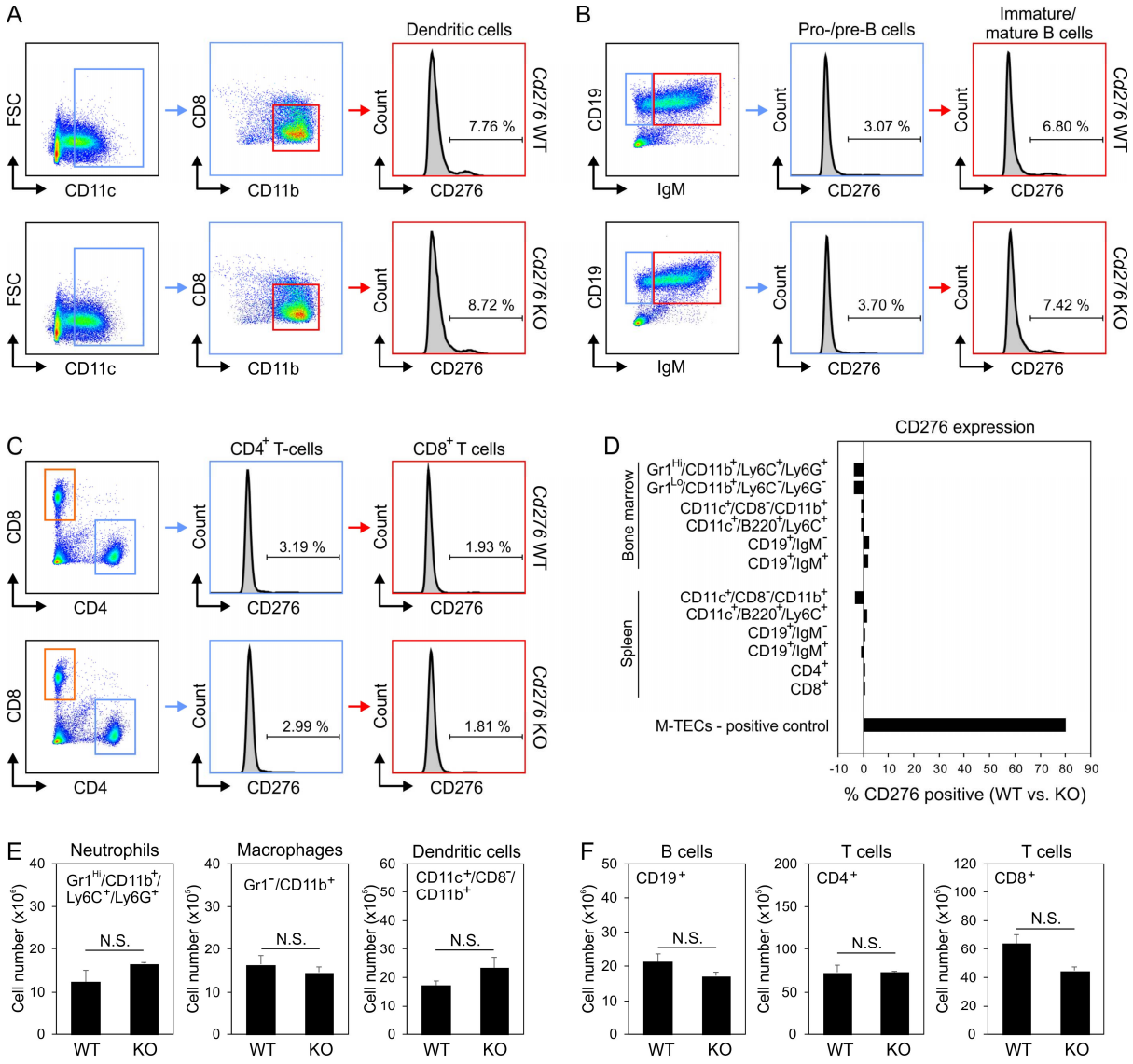

Figure S4, related to Figure 3. **(A-C)** m276-FITC binding to CD11c$^+$/CD8$^-$/CD11b$^+$ common dendritic cells (A) CD19$^+$/IgM$^-$ (pro-/pre-B cells) or CD19$^+$/IgM$^+$ (immature/mature) B cells (B) and CD4$^+$ or CD8$^+$ T cells (C) was evaluated by flow cytometry in *Cd276* WT and KO mice. **(D)** Flow cytometry with m276-FITC was used to evaluate CD276 expression on the indicated hematopoietic cell populations derived from bone marrow or spleen of *Cd276* WT versus KO mice. MC38-tumor endothelial cells (M-TECs) were used as a positive control and stained in parallel. The results shown are representative of six independent experiments. **(E, F)** Flow cytometry was used to evaluate total cell numbers of the indicated hematopoietic cell populations derived from the bone marrow (E) or spleen (F) of *Cd276* WT or KO mice following treatment with m276-MMAE. Mice were treated with 3 mg/kg m276-MMAE 6 times (biwk x 3) and bone marrow or spleen cells were harvested and analyzed 24 hours following the last treatment. Error bars in (E) and (F) = SD.

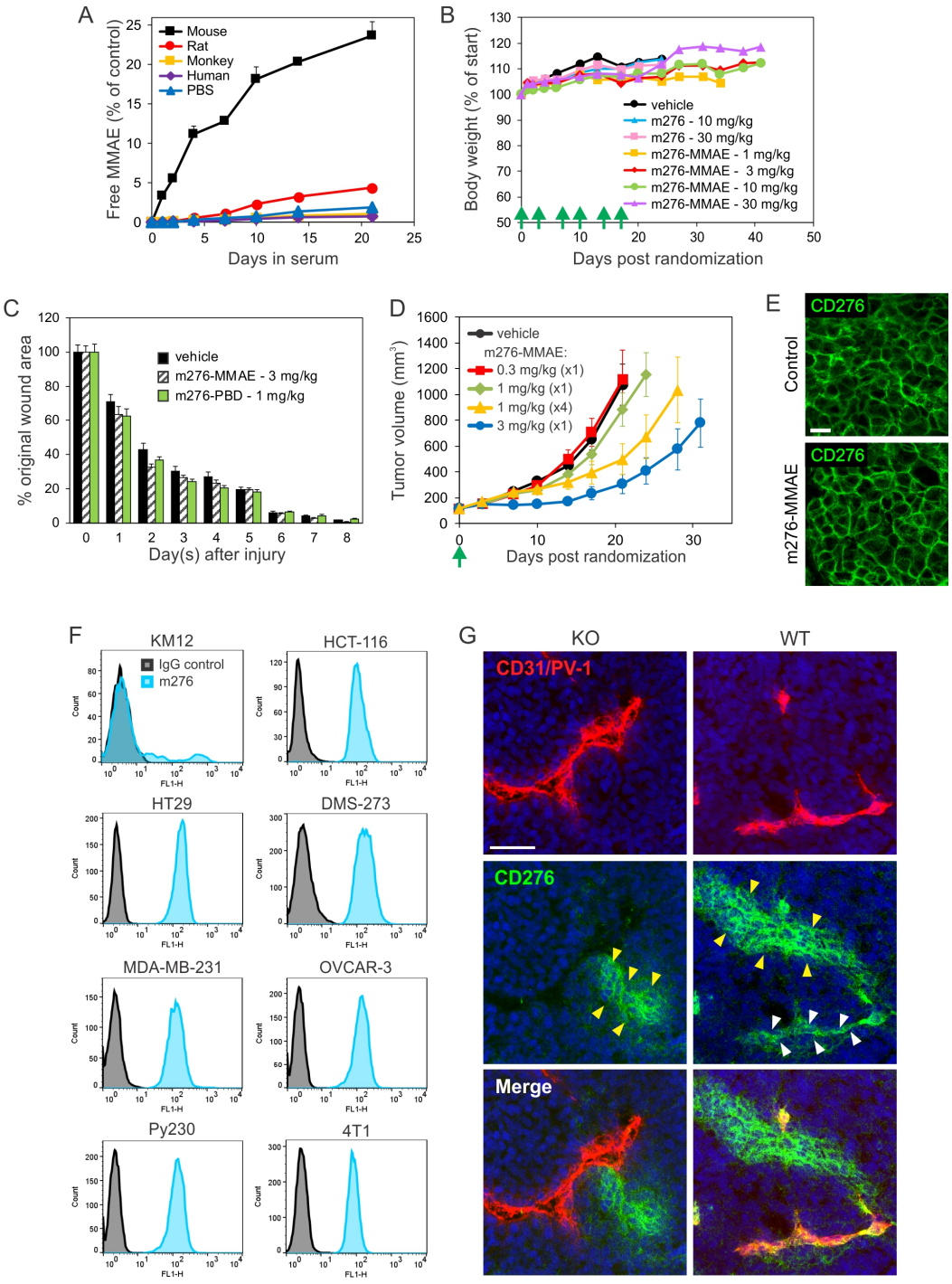

Figure S5, related to Figure 3. (A) Liquid chromatography-tandem mass spectrometry (LC-MS/MS) was used to evaluate m276-MMAE stability in serum from various species. Error bars = SD. **(B)** Body weights of mice in the HCT-116 tumor experiment in Figure 3D of main text. **(C)** Wound closure rates following treatment with m276-MMAE, m276-PBD or vehicle alone. n = 15 mice (30 wounds)/group. Error bars = SD. **(D)** The impact of a single dose of m276-MMAE (0.3, 1 or 3 mg/kg) was evaluated using MDA-MB-231 xenografts grown orthotopically in the mammary fat pad. In one of the groups a total of four doses of 1 mg/kg ADC was administered (biwk x 2). Treatments were initiated once tumors reached an average size

of ~100mm^3 (green arrow). n = 10 per group. Error bars = SEM. **(E)** CD276 immunofluorescence staining was performed on OVCAR3 control tumors and the relapsed tumors shown in Figure 3I (main text) that had been treated 23 times with m276-MMAE. Scale bar: 20μm. **(F)** Flow cytometry with m276 anti-CD276 was used to evaluate CD276 expression in various tumor cell lines. Note that KM12 cells displayed a low heterogeneous level of CD276 protein, and that m276 reacts with endogenous CD276 on both human (KM12, HCT-116, HT-29, DMS-273, MDA-MB-231, OVCAR-3) and murine (Py230 and 4T1) tumor cells. **(G)** Immunofluorescence staining of KM12 tumors. Note the small patches of CD276 positive tumor cells (yellow arrowheads) in both *Cd276* WT and KO mice, and CD276 positive tumor vessels (white arrowheads) only in *Cd276* WT mice. Tumor vessels were detected with a mixture of CD31 and Meca32 (PV-1) primary antibodies (red). Nuclei were counterstained with DAPI (blue). Scale bar: 50 μm.

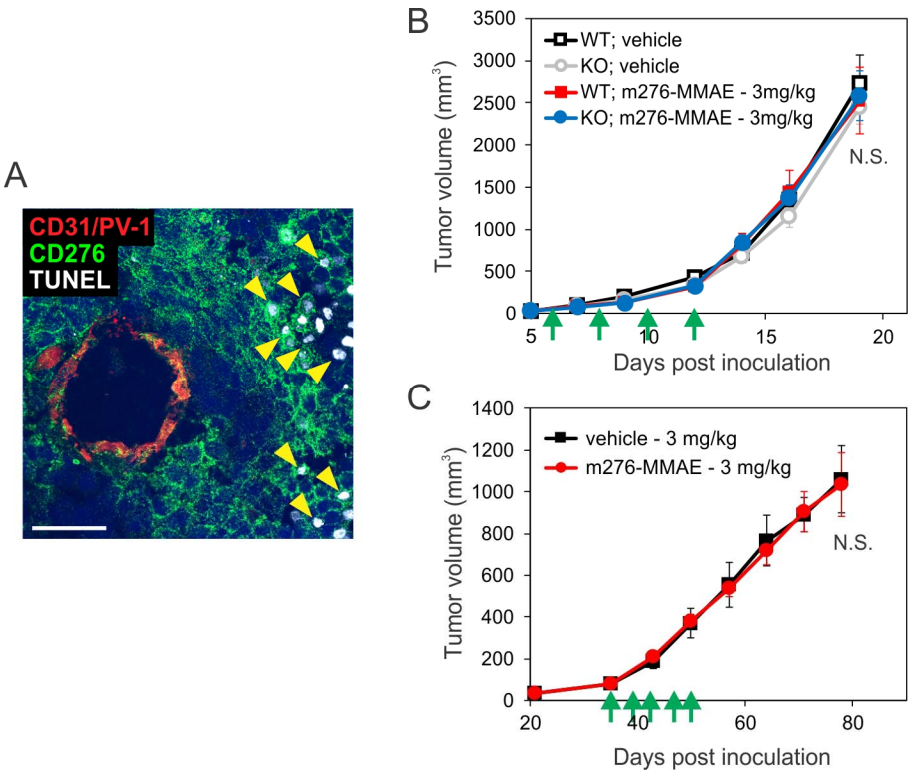

Figure S6, related to Figure 4. (A) Immunofluorescence staining was used to detect apoptotic cells (white) following treatment of KM12 tumors with m276-MMAE. To measure apoptosis, a TUNEL assay was used to detect DNA fragmentation (pseudocolored white). Arrowheads (yellow) point to TUNEL positive nuclei. Vessels were stained with a mixture of anti-CD31 and anti-PV1 (pseudocolored red). Note that m276-MMAE only induced apoptosis in the CD276 positive tumor cell patches (green). Scale bar: 50 μm. **(B)** MC38 tumor cells were inoculated subcutaneously into C57BL/6 *Cd276* WT or KO mice. Treatments (biwk x 2, green arrows) were initiated once tumors reached an average size of ~50 mm^3. n = 16 mice/group. **(C)** Pan02 tumor cells were inoculated subcutaneously into C57BL/6 *Cd276* WT or KO mice. Treatments (biwk x 2, green arrows) were initiated once tumors reached an average size of ~90 mm^3. n = 13 mice/group. Error bars in (B) and (C) represent SEM. N.S.: No significant difference between any of the groups.

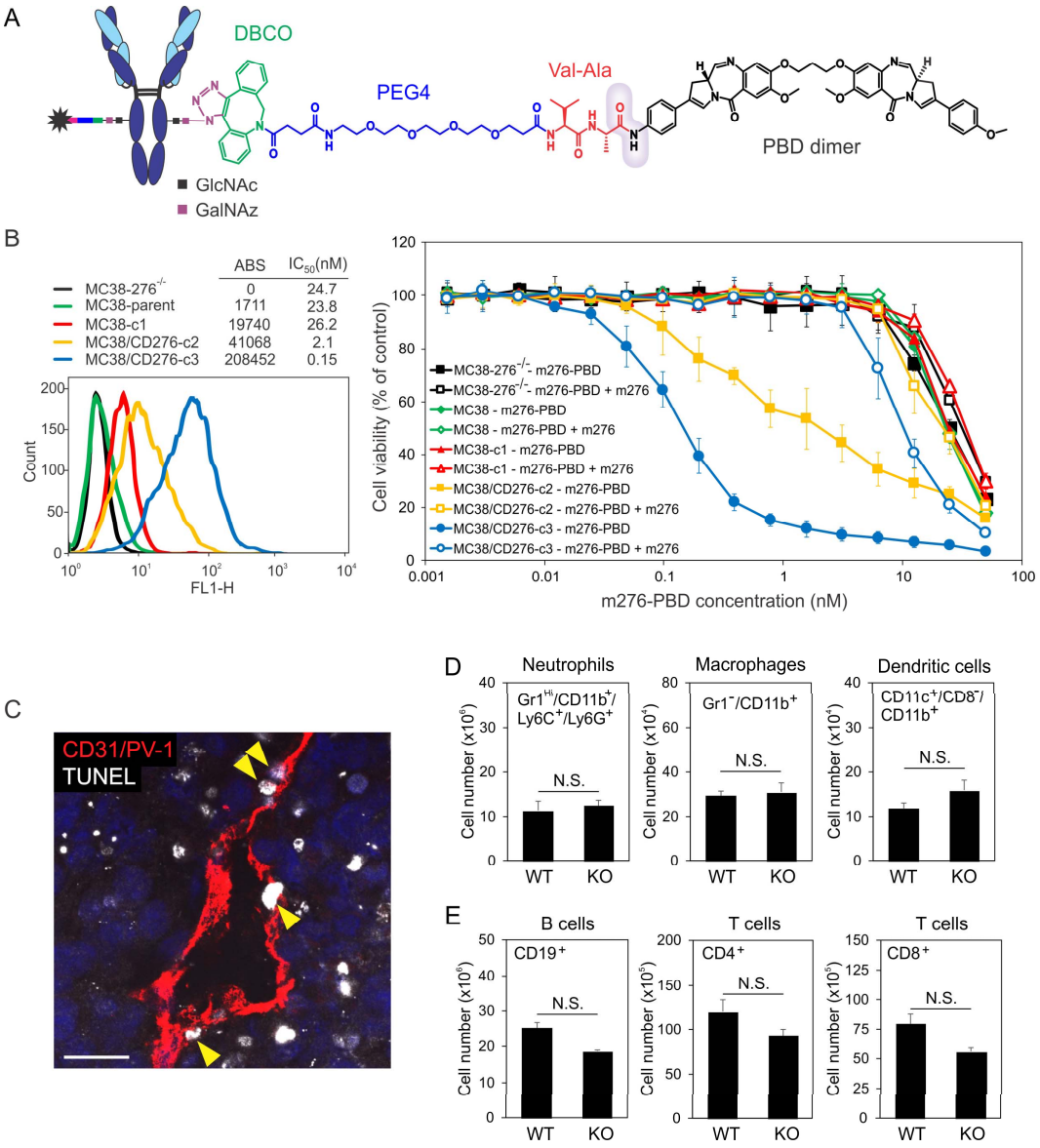

Figure S7, related to Figure 6. (A) Chemical structure of m276-PBD linker and warhead. The dibenzylcyclooctyne (DBCO) attachment group is in green, a 4-unit polyethylene glycol (PEG4) spacer is in blue, and a cathepsin B cleavable valine-alanine dipeptide is in red. The PBD-drug linker was bound to m276 via a 2-azido-galactose (GalNAz) glycol group. The grey cloud highlights the amide group potentially susceptible to cleavage by carboxylesterase 1C in mouse serum. **(B)** Left panel: Flow cytometry quantification of CD276 antibody binding sites (ABS) on MC38 parent cells, MC38 *Cd276* null cells (MC38-276$^{-/-}$) or three clones expressing increasing amounts of CD276. Right panel: Cell viability of MC38 cells treated with m276-PBD. IC_{50} values for the m276-PBD treated samples are shown in the left panel. Specificity of m276-PBD for CD276 was assessed by competing each cell line with an excess of unlabeled m276 antibody (open symbols). **(C)** Immunofluorescence TUNEL staining was used to detect apoptotic cells (pseudocolored white) following treatment of MC38 tumors with m276-PBD. Arrowheads (yellow) point to TUNEL positive vessel nuclei. Scale bar: 20 µm. **(D-E)** Flow cytometry was used to evaluate total cell numbers of the indicated hematopoietic cell populations derived from the bone marrow (D) or spleen (E) of *Cd276* WT or KO mice following treatment with m276-PBD. Mice were treated with 1 mg/kg m276-PBD 4 times (biwk x 2) and bone marrow or spleen cells were harvested and analyzed 24 hours following the last treatment. Error bars in (B), (D) and (E) = SD.